BOND BEHAVIOUR OF FRP FOR PURE AXIAL TENSION STRENGTHENING OF CONCRETE

Junrui Zhang, University of Auckland, New Zealand, junrui.zhang@auckland.ac.nz
Ravi Kanitkar, KL Structures, USA, ravi@klstructures.com
Enrique del Rey Castillo, University of Auckland, New Zealand, e.delrey@auckland.ac.nz
Kent A. Harries, University of Pittsburgh, USA, kharries@pitt.edu
Rhys Rogers, RAC Consulting, New Zealand, rhys.rac@outlook.com
Aniket Borwankar, Simpson Strong-Tie, USA, aborwankar@strongtie.com

ABSTRACT
Designing fibre reinforced polymer (FRP) for pure axial tension strengthening has relied on guides primarily based on small-scale single lap shear tests. Recent tests with longer lengths of multi-layered FRP appear to indicate that the peak debonding failure load is primarily influenced by stiffness of the FRP and that effective bond lengths may exceed the predictions from current guides. In addition, it appears that the bonded length does not affect the peak force. The tests reveal that fibre anchors can help to control debonding and increase tensile capacity. The paper summarizes the testing results and discusses the implications on design.

KEYWORDS
FRP strengthening; fibre anchors; debonding; bond length

INTRODUCTION
FRP materials are known for their high strength-to-weight ratio, corrosion resistance, and ease of installation, making them ideal for use in structural strengthening applications. Numerous studies have evaluated the effectiveness of FRP composites in strengthening various types of concrete structures such as beams, columns, and slabs (Lam and Teng, 2003; El-Ghandour, 2011; del Rey Castillo et al., 2018). At present, the available design guidelines limit the effectiveness of FRP on the basis of the strain at which it is expected to debond from the concrete substrate. This is reasonable since debonding occurs at a much lower strain in the FRP when compared to its ultimate failure strain. The bond behaviour of FRP has been extensively studied for common strengthening applications such as beam flexure and shear and the available design guidelines appear to capture the effectiveness of FRP reasonably well for such applications. Pure tensile strengthening of concrete with long lengths of thick/stiff FRP is becoming more accepted, e.g., when internal reinforcement providing continuity or prestress is compromised or for seismic strengthening of diaphragms. The design of FRP pure axial tensile strengthening often relies on provisions from guidelines such as PRC ACI 440.2-17, CNR DT-200, and fib bulletin 90, which are based on small-scale single lap shear tests that primarily only capture end debonding. These lap tests with short (250 mm long or less) and thin (1 mm thick or less) FRP strips do not resemble the much longer and thicker (multi-layered) strips used in practice. Available testing with fibre anchors typically only includes small anchors with shallow embedment depths which are not representative of the current state of practice. As a result, there is considerable uncertainty in the industry regarding the design of FRP to strengthen concrete structures for pure axial tension and about the effectiveness of fibre anchors.

The aim of this study is to investigate the debonding behaviour of multi-layered long FRP strips and evaluate the influence of fibre anchors. Recent research findings (del Rey Castillo et al. 2022) suggest that various factors have an impact on the behaviour of these strips. For instance, the load carrying capacity is notably influenced by the thickness of the FRP strips, while the length of the FRP strips affects the post-debonding performance of the FRP. Fibre anchors effectively help control debonding and enhance the tensile capacities of the FRP. The authors also proposed a hypothetical force-

displacement behaviour of anchored FRP strips (del Rey Castillo et al, 2022). The test program described in this paper was designed to test this hypothesis.

EXPERIMENTAL PROGRAM
The experimental program was designed to evaluate the interfacial bond behaviour of thick (stiff) and long FRP strips bonded to concrete. A total of 60 specimens, consisting of 36 specimens with unanchored FRP and 24 specimens with anchored FRP, were tested. The mechanical properties of the FRP system were assessed using 42 coupon tests tested in accordance with ASTM D3039. Compressive strength of the concrete was obtained from cylinders taken during the concrete placement and tested per ASTM C-39. The resulting nominal concrete strengths are listed in the test matrices. The experimental study presented was carried out using US units; the specimen identification reflects this. In this paper all data has been presented in equivalent SI units.

The FRP reinforcement system used in the test program is the Simpson Strong-Tie CUCF11 FRP fabric, with an areal weight of 370 g/m^2 and a nominal laminate thickness, t_f, of 0.5 mm. This FRP reinforcement has a design tensile strength of 883 MPa and a mean elastic modulus, E_f, of 98 GPa. The fibre anchors are the CSS-PCA with a precured portion for insertion and embedment into the concrete blocks and a free-fibre end for saturation with epoxy and for bonding bond to the FRP reinforcement. The fibre anchors are manufactured from the same constituent materials as the FRP fabric. Single-lap shear tests using static monotonic loading were used to characterize the bond behaviour of the FRP-concrete interface. A load frame was used to securely anchor the concrete blocks, while a servo-hydraulic actuator applied direct tension force to the FRP strip(s). A conceptual setup of the tests is shown in Figure 1. The test matrices, including relevant details, can be found in Table 1and Table 2.

Table 1: Unanchored FRP test matrix

Configuration / Bonded length	305 mm	610 mm	914 mm
1 layer (t_f = 0.5 mm)	1	1	1
2 layers (t_f = 1.0 mm)	1	1	1
3 layers (t_f = 1.5 mm)	1	1	1
4 layers (t_f = 2.0 mm)	1	1	1

Each unanchored FRP configuration was tested with three different concrete compressive strengths, namely 17.2, 20.7 and 34.5 MPa. For all tests the width of the FRP strip was maintained at 152 mm. Only one test was conducted for each set of parameters and concrete strength.

Table 2: Anchored FRP test matrix

| Configuration / Fibre anchor diameter	13 mm	19 mm	25 mm
One anchor (l_f = 203 mm), 1 layer	1	1	1
One anchor (l_f = 406 mm), 1 layer	1	1	1
Two anchors (l_f = 305 mm, s_a = 305 mm), 2 layers	1	1	1
Two anchors (l_f = 305 mm, s_a = 610 mm), 2 layers	1	1	1

Each anchored FRP configuration was tested with two different concrete compressive strengths, namely 17.2 MPa and 34.5 MPa. For the fibre anchors, l_f indicates fan or splay length and s_a represents the spacing of anchors. The width of the FRP strip was maintained at 152 mm for all the tests and the total bonded length was 1220 mm. Only one test was conducted for each set of parameters and concrete strength.

Prior to the installation of the FRP strips, the concrete surface was ground to achieve the desired profile, and anchor holes, if applicable, were drilled and the edges were rounded. Epoxy putty was

used to fill small bug holes and the surface was primed with neat resin. The carbon fabrics were cut to the desired width and length, saturated with epoxy resin, and placed onto the prepared concrete surface. The predrilled anchor holes were filled with epoxy resin, and the free fibre end of the pre-cured anchors was saturated with epoxy resin. The anchors were then installed into the epoxy-filled holes, the splays were adhered to the first layer of FRP, and then the second layer of FRP was installed to sandwich the FRP anchor fans. After curing at a temperature of 27 Celsius degrees for at least four days, a black and white speckled paint pattern was applied for the digital image correlation (DIC) system to work, and the specimens were tested. Figure 1(a) and (b) illustrate the representative specimens utilized in the experimental program. At the loaded end of the strips, the FRP was left unbonded for 152 mm to prevent concrete edge breakout. As shown in Figure 2, a vertical load frame securely anchored the specimens, while a servo-hydraulic actuator applied tensile loading to the FRP strip, The loading rate of 0.1 in./min [2.54 mm/min] was used during the testing procedure. The specimens were restrained vertically and braced laterally during loading. Load and actuator displacement data were recorded by a load cell, and a 3D optical deformation measurement digital image correlation (DIC) system was used to capture the displacements and strains on the surface of the FRP during the tests. The DIC analysis is not presented in this paper, and a comprehensive study using DIC analysis will be published later.
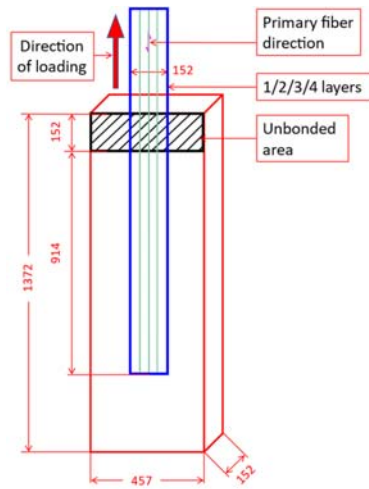
1(a) Unanchored FRP Specimens (multiple layers of FRP)
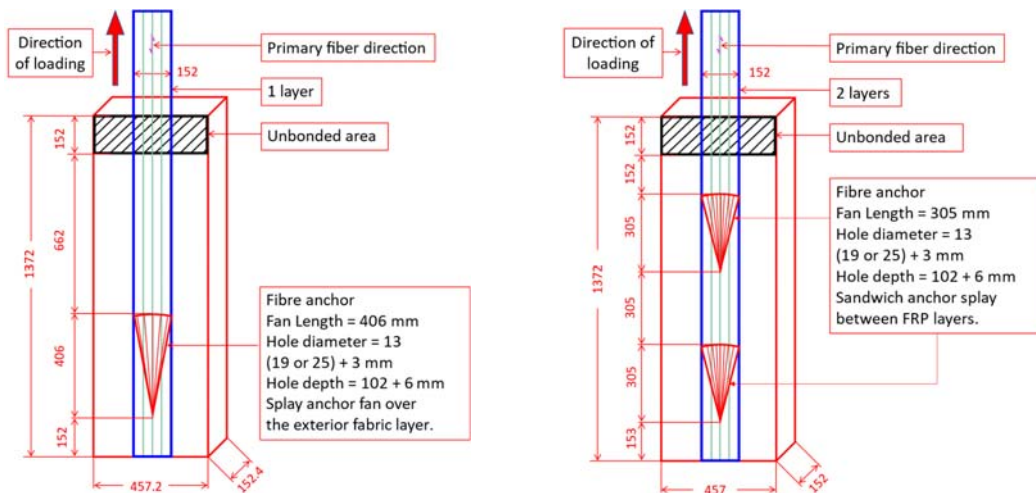
One-anchor specimen (one layer of FRP)   Two-anchor specimen (two layers of FRP)

1(b) Anchored FRP Specimens

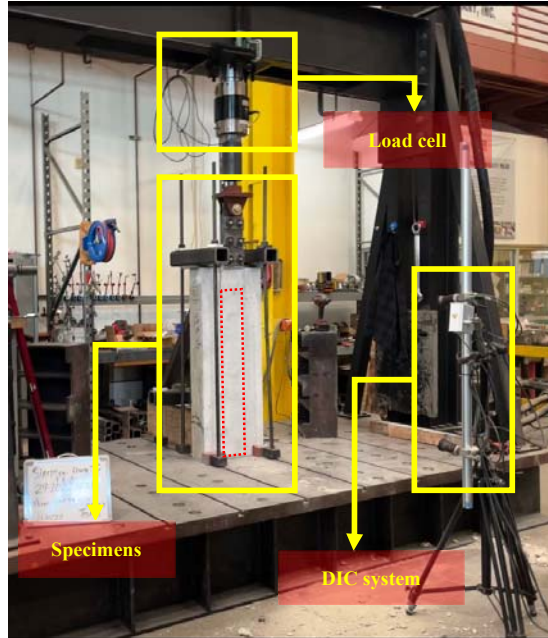Figure 1: Typical specimen configuration

3

Figure 2: Typical experimental setup

For the two-anchor specimens, the anchors were placed after the first FRP layer was installed, and the anchor splay was sandwiched between the two layers. The two-anchor specimen shown in Figure 1(b) represents the case where the anchor spacing is 610 mm. Another configuration used a spacing of 305 mm, wherein the top anchor was closer to the bottom anchor and the splay of the bottom anchor was at the same level as the drilled hole for the top anchor.

RESULTS AND DISCUSSION
For each test, the load and the displacement of loaded end of the FRP strip were recorded. In addition, the DIC data was also recorded for a detailed analysis of the debonding behaviour of the FRP and the anchors. The experimental results are described below for both the unanchored and anchored FRP tests.

Tests of unanchored FRP strips
As described in Table 1, a series of unanchored FRP strips were tested with different layers for different concrete strengths. The intent of this testing was to capture the interaction between the stiffness ($E_f t_f$) of the FRP and the concrete strength. It is well understood from literature that as the FRP stiffness increases, the debonding strain reduces. The current design guidelines indicate that as concrete strength increases so does the strain at which debonding occurs.

Failure modes
All unanchored FRP strips exhibited debonding of the FRP from the concrete as the primary failure mode, with the FRP detaching from the concrete with a thin layer of concrete attached to it. Three of the tests failed prematurely as a result of installation or test setup errors. These three tests are omitted from further discussion. The premature failures were caused primarily by a very slight misalignment of the loading steel plate and the concrete, resulting in an eccentricity that caused premature FRP fracture above the unbonded length and at the edge of the concrete. In the next phase, such alignment issues will be mitigated to more appropriately represent the planar forces expected in the FRP. Table 3 presents the peak debonding force, *Nd*, for each of the unanchored tests.

Table 3: Peak debonding force for unanchored FRP Tests

| Test ID	concrete strength	bonded length	layers	N_d	Test ID	concrete strength	bonded length	layers	N_d
	MPa	mm	#	kN		MPa	mm	#	kN
2500-12-1	17.2	305	1	30.5	3000-24-3	20.7	610	3	53.0
2500-12-3	17.2	305	3	58.0	3000-24-4	20.7	610	4	61.7
2500-12-4	17.2	305	4	61.7	3000-36-2	20.7	914	2	49.7
2500-24-1	17.2	610	1	26.4	3000-36-3	20.7	914	3	56.3
2500-24-2	17.2	610	2	47.2	3000-36-4	20.7	914	4	60.3
2500-24-3	17.2	610	3	41.1	5000-12-1	34.5	305	1	38.4
2500-24-4	17.2	610	4	55.8	5000-12-2	34.5	305	2	51.0
2500-36-1	17.2	914	1	31.9	5000-12-3	34.5	305	3	59.0
2500-36-2	17.2	914	2	43.3	5000-24-1	34.5	610	1	36.5
2500-36-3	17.2	914	3	45.5	5000-24-2	34.5	610	2	51.8
2500-36-4	17.2	914	4	55.5	5000-24-3	34.5	610	3	63.7
3000-12-1	20.7	305	1	38.3	5000-24-4	34.5	610	4	63.4
3000-12-2	20.7	305	2	40.3	5000-36-1	34.5	914	1	37.5
3000-12-3	20.7	305	3	58.6	5000-36-2	34.5	914	2	45.9
3000-12-4	20.7	305	4	65.0	5000-36-3	34.5	914	3	59.7
3000-24-1	20.7	610	1	29.8	5000-36-4	34.5	914	4	65.8
3000-24-2	20.7	610	2	41.4					

Load-Displacement curves

Figure 3 shows force-displacement curves for two bonded lengths, namely 305 mm and 915 mm, for each concrete compressive strength (specimens indicated with a red star experienced a premature failure due to setup or installation errors). Figure 3 clearly shows that, as expected, as the number of FRP layers (stiffness) increases, the force developed at debonding also increases. However, Figure 3 also indicates that over the range of different compressive strengths, the peak debonding force does not vary significantly with a change in the bonded length for a given FRP stiffness. For example, for the 34.5 MPa concrete, 1 layer of FRP has a peak debonding force of 38.4 kN for a 305 mm bonded length and 37.5 kN for a 915 mm bonded length. The longer FRP strips appear to show a plateau, or a continued load-carrying capacity, beyond the peak debonding load while for the shorter lengths the failure is relatively sudden after reaching the peak debonding load. This plateau can be attributed to a longer available length past the location of initial debonding and can be thought of an effective bond length that progresses from the loaded end of the strip till the free end is reached. These observations will have to be confirmed by performing multiple tests for each set of parameters, but the trends are quite similar over this limited experimental effort.
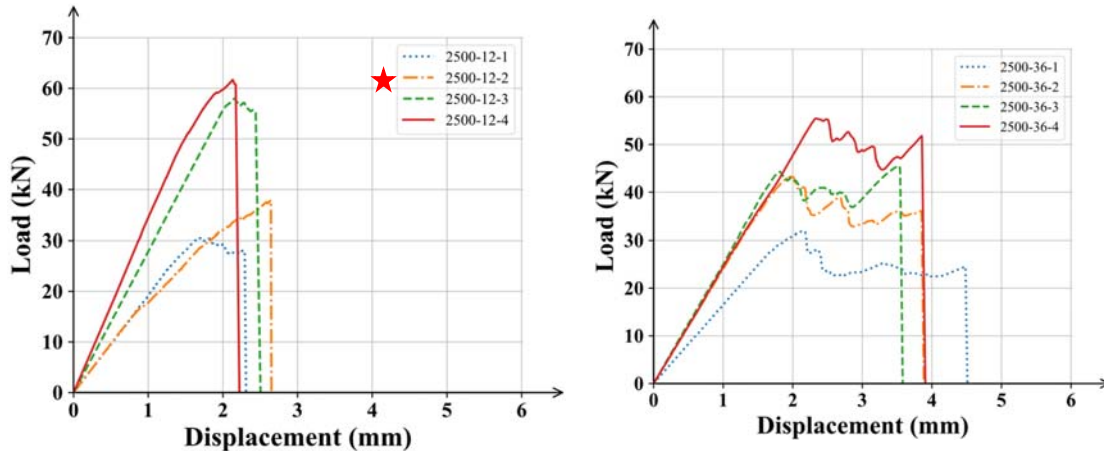
3(a) Force-displacement for 305 mm (left) & 915 mm (right) bonded length and f'$_c$ = 17.2 MPa
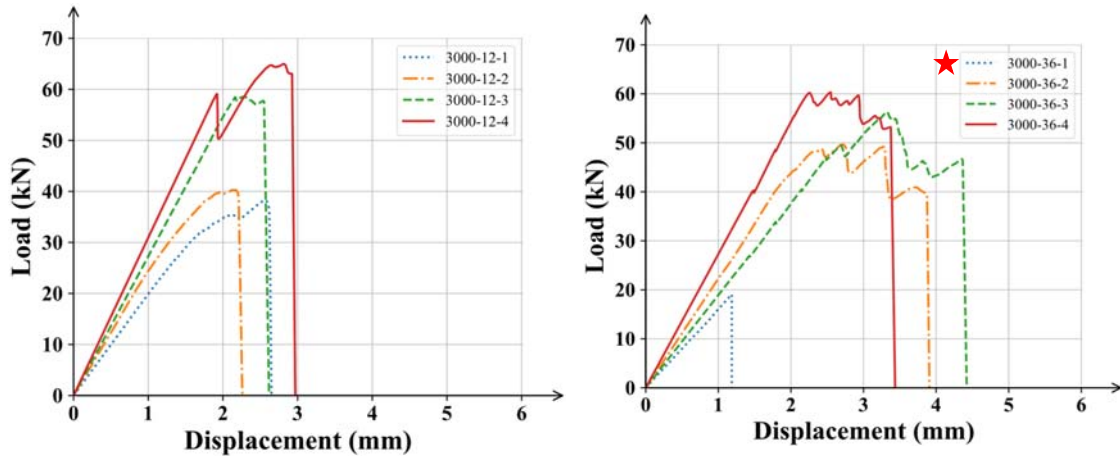
3(b) Force-displacement for 305 mm (left) & 915 mm (right) bonded length and f'_c = 20.7 MPa
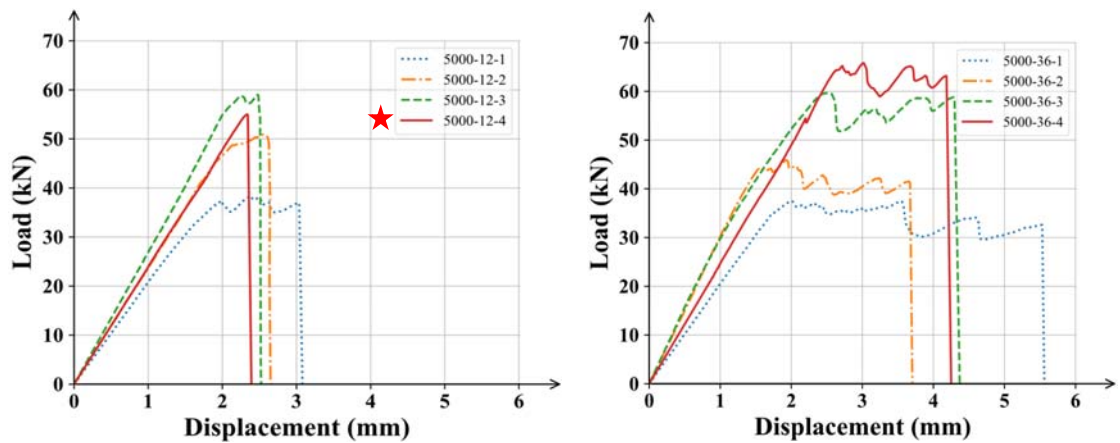
3(c) Force-displacement for 305 mm & 915 mm bonded length and f'_c = 34.5 MPa

Figure 3: unanchored FRP – force-displacement plots

Tests of anchored FRP strips

The intent of the anchored FRP strips was to observe if and how the anchors, including the length of the splay and the spacing between the anchors, modified the failure mode of the FRP strips. It was hypothesized that anchors would be effective in controlling the debonding failure mechanism and allow higher loads to be developed. The anchors were designed to allow the strips to reach their full tensile strength using the design methodology outlined in del Rey Castillo et al 2019 and the expected failure mode was FRP strip rupture.

Failure modes

The anchored FRP strips exhibited a variety of failures at the peak debonding load. The initial performance of the anchored strips was similar to the unanchored strips with debonding of the FRP at the loaded end. However, once the debonding reached the anchor splays, the anchors were engaged and allowed the load to increase. For the one-anchor tests, the failure was due to either a debonding of the anchor splay from the FRP strip, anchor rupture or rupture of the FRP strip. The debonding of the anchor splay from the FRP was observed only for the one-anchor tests, where the anchor splay was bonded only on side to the FRP strip. The debonding failure was unexpected and is attributed to poor installation. For the two-anchor specimens, the debonding eventually continued past the first anchor and caused the second anchor to be engaged. Except one test which failed by debonding of the splay from the FRP, all the two-anchor specimens failed in rupture of the FRP strips. One two-anchor specimen (5000-2-24-12-1) failed prematurely due to an unexpected slip in the loading mechanism and is not considered to be representative of FRP behaviour. It should be noted that for many of the anchored tests the FRP rupture occurred at the edge of the loading assembly leading to a large

6

variation in the peak force. This is attributed to errors in alignment which likely resulted in bending of the FRP strip near the loading rig. However, this variation in peak load does not adversely affect the outcome of this effort since the objective is to assess the change in performance of the FRP due to the addition of anchors. Table 4 presents the peak debonding force, N_d, for each of the anchored tests. The calculated expected tensile strength of one layer for the FRP strip is approximately 80 kN, while that for two layers is approximately 160 kN. It can be observed that in most of the tests the FRP ruptured at loads below these expected tensile strengths due to the alignment issues discussed above.

Table 4: Peak debonding force for anchored FRP Tests

Test ID	Concrete strength	Anchor's number	Anchor's spacing	Dowel's diameter	N_d (kN)	Failure Mode[1]
2500-1-0-8-0.5	17.2	1	NA	13	62.7	FD
2500-1-0-16-0.5	17.2	1	NA	13	64.2	AR
2500-2-12-12-0.5	17.2	2	305	13	131.4	FR
2500-2-24-12-0.5	17.2	2	610	13	130.0	AR
2500-1-0-8-0.75	17.2	1	NA	19	71.0	FD
2500-1-0-16-0.75	17.2	1	NA	19	65.0	FD
2500-2-12-12-0.75	17.2	2	305	19	97.5	FR
2500-2-24-12-0.75	17.2	2	610	19	125.7	FR
2500-1-0-8-1	17.2	1	NA	25	76.7	FR
2500-1-0-16-1	17.2	1	NA	25	57.0	FR
2500-2-12-12-1	17.2	2	305	25	127.6	FR
2500-2-24-12-1	17.2	2	610	25	129.6	FR
5000-1-0-8-0.5	34.5	1	NA	13	58.5	FR
5000-1-0-16-0.5	34.5	1	NA	13	75.7	FR
5000-2-12-12-0.5	34.5	2	305	13	128.7	FR
5000-2-24-12-0.5	34.5	2	610	13	131.3	FR
5000-1-0-8-0.75	34.5	1	NA	19	66.2	FR
5000-1-0-16-0.75	34.5	1	NA	19	66.8	FD
5000-2-12-12-0.75	34.5	2	305	19	135.2	FR
5000-2-24-12-0.75	34.5	2	610	19	149.6	FR
5000-1-0-8-1	34.5	1	NA	25	76.9	FR
5000-1-0-16-1	34.5	1	NA	25	80.1	FR
5000-2-12-12-1	34.5	2	305	25	141.5	FR
5000-2-24-12-1	34.5	2	610	25	107.2	SF

[1]Failure modes: FD = anchor fan debonding, FR = fabric rupture, AR = anchor rupture, SF = failure mode related to setup, installation etc.

Load-Displacement curves
Figure 4 shows force-displacement curves for the different tests. Figure 4a shows the force-displacement plots for one-anchor tests for the two different concrete strengths. The left-hand plot is for the shorter anchor splay of 203 mm while the right-hand plot is for the longer splay of 406 mm. It can be observed that the debonding is initiated at approximately same load for all the specimens. It can also be observed that force at which debonding is initiated is similar in the anchored FRP tests and the unanchored FRP tests for the same concrete compressive strength. Once debonding starts it progresses along the strip till the anchor is engaged. This progression results in a small plateau as the displacement increases without a significant change in the force. The anchor resists the applied load leading to an increase in the stiffness of the system as well as the load-carrying capacity. In design, the ratio of the area of fibre in the anchors relative to the area of fibre in the anchored strip is an important consideration. For the 13, 19 and the 25 mm anchors, the ratio is 1.58, 3.67 and 6.54.

Anchor splay length = 203 mm

4(a) Force-displacement for one-anchor tests and f'_c = 17.2 & 34.5 MPa

Anchor splay length = 406 mm

Anchors spaced at 305 mm

Anchors spaced at 610 mm

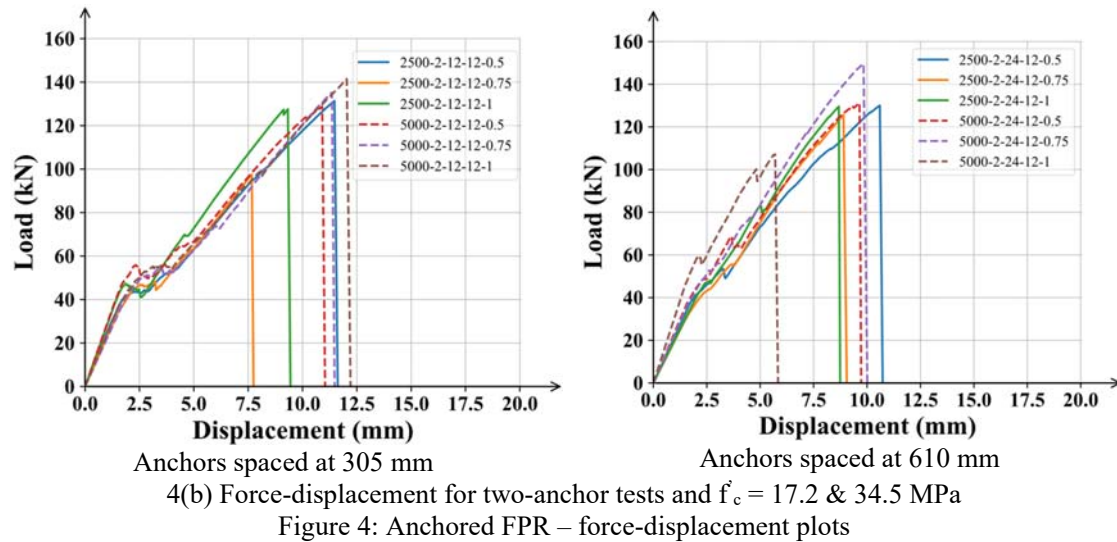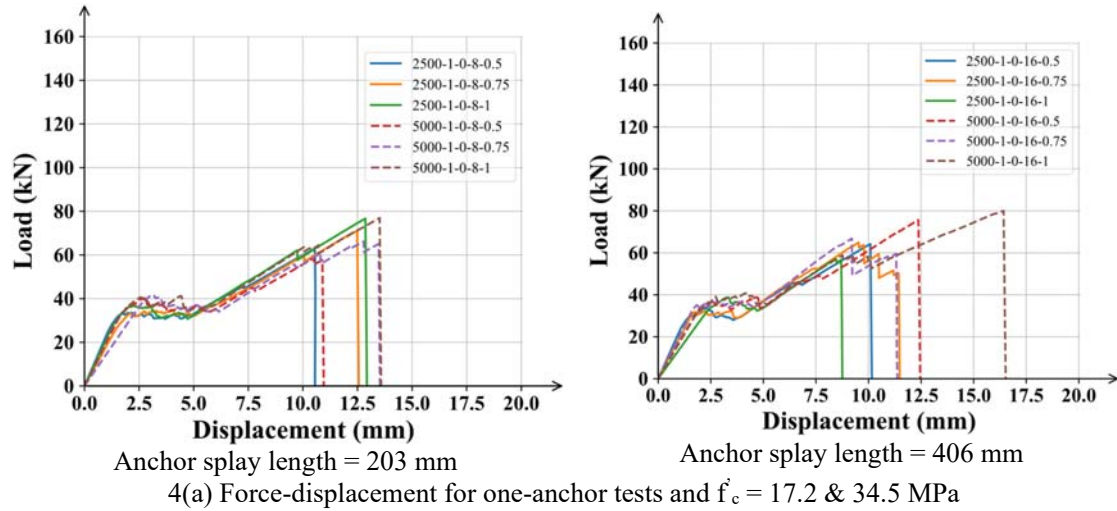4(b) Force-displacement for two-anchor tests and f'_c = 17.2 & 34.5 MPa

Figure 4: Anchored FPR – force-displacement plots

Figure 4(b) shows that the two-anchor specimens exhibit a similar behaviour to the one-anchor specimens. The load at which debonding is initiated is similar to the one-anchor tests. Since the first anchor is much closer to the loaded end, the plateau is much shorter before the anchors are engaged. The plateau length appears to be proportional to the debonded length of the FRP between the loaded end and the first anchor. For both spacings of 305 mm and 610 mm, it appears that both anchors are engaged at essentially the same time and the resulting peak load is about twice that from the one-anchor tests. This indicates that the fibre anchors undergo some deformation and allow the debonding to extend past the first anchor to activate the second anchor. The behaviour may be different if the spacing between the anchors is larger than the 610 mm maximum spacing used in these tests. Once the DIC data is analysed, the progression of debonding along the strips, between the anchors, and the resulting stress in the strips will be better understood.

As mentioned earlier, the authors based this testing program on a hypothesized force-displacement behaviour of anchored FRP strips (del Rey Castillo et al, 2022) shown in Figure 5(a).

8
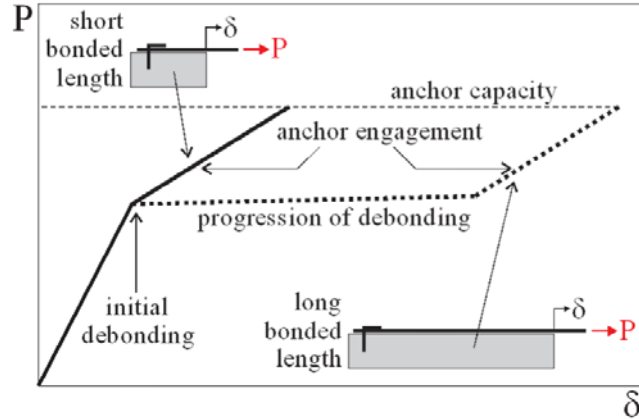
5(a) Proposed hypothetical behaviour of anchored FRP strips
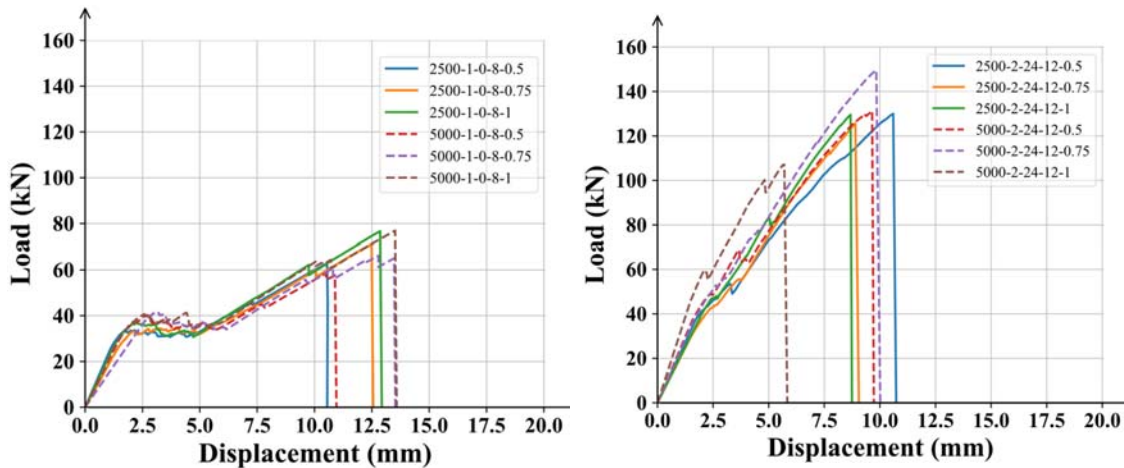
5(b) Experimental behaviour of long and short bonded length conditions
Figure 5: Behaviour of anchored systems

The left-hand plot in Figure 5(b) represents the condition wherein a longer bonded length is available between the loaded end and the fibre anchor (one-anchor specimens). The right-hand plot in Figure 5(b) represents the condition wherein only a short length is available between the loaded end and the fibre anchor (two-anchor specimens). It is noted that the observed behaviour agrees well with the proposed hypothesis. The authors hope to develop a better understanding of the behaviour of anchor FRP strips in pure tension so as to appropriately design future experimental programs.

Comparison to design guidelines
The commonly used FRP design guides, such as fib Bulletin 90 and PRC ACI 440.2-17, provide for calculating the tensile strength of concrete strengthened with FRP. None of the available design guides address the use of fibre anchors. As mentioned above, these provisions are based on single lap shear testing performed with relatively thin and short FRP strips. The applicability of the available provisions to long and thick unanchored FRP strips for pure tensile strengthening is not well understood. Figure 6 shows a comparison of the test results from this effort to those calculated from the design level equations (95% percentile values) of fib Bulletin 90 provisions for debonding at intermediate cracking (IC) and PRC ACI 440.2-17 Section 12.4 for pure tension strengthening.

The peak debonding load calculated from the fib Bulletin 90 IC debonding equations appears to be unconservative for some of the specimens. The calculated peak load from ACI 440.2-17 Section 12.4 appears to generally be adequately conservative for all the tested specimens. More investigation is required to determine the applicability of the design codes to such applications, especially the sensitivity of the peak load to the concrete compressive strength. The authors are currently reviewing

9

the data from this effort in conjunction with the data for short bonded lengths available in the literature to investigate the provisions in the design guidelines.
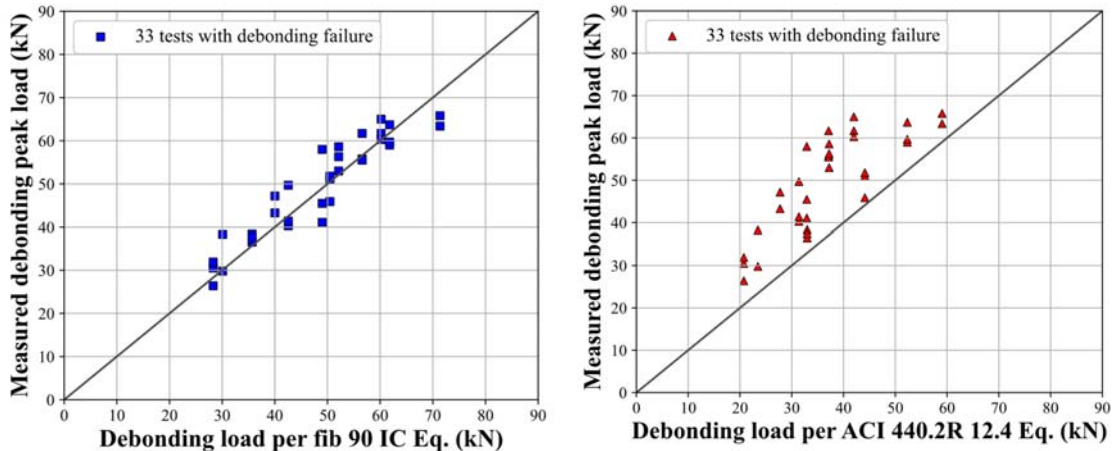

Figure 6: Unanchored FRP Strip: measured versus calculated peak debonding load

OBSERVATIONS & CONCLUDING REMARKS

This experimental program was conducted to investigate the debonding behaviour of long multilayered FRP strips in strengthening concrete under pure axial tension and to evaluate the influence of fibre anchors. In addition, the authors hoped to develop a better understanding of how anchored FRP strips perform as the location and the spacing between anchors is varied.

- As expected, the unanchored FRP strips failed by debonding of the FRP from the substrate. For the anchored strips, the initial debonding load was similar to that for the unanchored strips, but the fibre anchors enabled the FRP to achieve significantly higher peak loads even though the FRP strip was essentially fully debonded from the substrate. The failure of the anchored strips was primarily by either anchor or FRP rupture.
- For the unanchored FRP strips, the length of the FRP strips does not affect the peak debonding load, but it does influence the force-displacement behaviour, with shorter lengths resulting in a rapid drop in load and longer lengths leading to a plateau, or a continued load-carrying capacity to higher displacements. This is attributed to a progression of debonding from the loaded end to the free end of the strip.
- Although higher peak debonding load is observed as the compressive strength of the concrete substrate increases, the overall effect appears to be smaller than expected from the design guides. For example, doubling the compressive strength, from 17.2 MPa to 34.5 MPa, leads to an average increase in peak debonding load of about 122%. This effect needs to be studied in more detail with more tests of each set of parameters.
- As expected, the presence of fibre anchors does not significantly affect the initial debonding load. Once the debonding reaches the fibre anchors, the anchors control FRP debonding and add tensile strength to the system. Once the progressive debonding reaches an anchor, the anchor engages via the bond between the FRP and the splay. The stiffness of the system increases quickly as the anchor starts to resist the load being applied.
- For FRP strips with two anchors spaced as far as 610 mm, it was observed that the debonding was able to progress beyond the first anchor and engage the second anchor almost simultaneously so that both anchors contributed to the total tensile capacity. This is attributed to some flexibility of the anchor. It is not clear if the same behaviour will be observed if the FRP strips are thicker or if the anchors are placed further apart. Sandwiching an appropriately detailed anchor splay between FRP layers appears to mitigate the debonding of the splay from the FRP and results in either anchor rupture or FRP strip rupture.

- DIC analysis of the tests will be conducted to better understand the progression of debonding along the FRP strips. Such a detailed analysis will aid in better understanding the effective bond length for longer FRP strips and its variation from the typical short strips previously studied by other researchers.
- This test program was able to validate the hypothetical behaviour developed by the authors for anchored FRP strips and presented in a previous paper. The authors hope to extend this understanding of anchored FRP by designing suitable specimens for the next phase of experimental work.

ACKNOWLEDGEMENT
The authors acknowledge the invaluable assistance of Mike Lin, Griff Shapack, Mike Wesson and other members of the Tye Gilb Laboratory, Simpson StrongTie in Stockton, California, in the preparation and testing of the specimens.

CONFLICT OF INTEREST
The authors declare that they have no conflicts of interest associated with the work presented in this paper.

DATA AVAILABILITY
Data on which this paper is based is available from the authors upon reasonable request.

REFERENCES

ACI, Guide for the Design and Construction of Externally Bonded FRP Systems for Strengthening Concrete Structures. *PRC ACI 440.2 (2017)*, Farmington Hills, Michigan, USA.

Fib Bulletin 90, Externally Applied FRP Reinforcement for Concrete Structures (2019). *Federation Internationale de Beton (fib)*, Lausanne, Switzerland

Del Rey Castillo, E., Kanitkar, R., Harries K., Rogers, R. (2022). Applicability of fib Bulletin 90 Chapter 5 to Real Life FRP Design. *Proceedings of 6th fib International Congress* in Oslo, Norway.

Del Rey Castillo, E., Kanitkar, R., Smith, S. T., Griffith, M. C., Ingham, J. M. (2019). Design approach for FRP spike anchors in FRP-strengthened structures. *Composite Structures*. 214 (2019) 23-33.

Del Rey Castillo, E., Harries K., Rogers, R., Kanitkar, R. (2022). FRP tension ties: State-of-the-art review of existing design guidance for debonding capacity and applicability to concrete diaphragm seismic strengthening. *Journal of Composites in Construction*, Vol. 26, No. 2, p. 04022014.

Del Rey Castillo, E., Griffith, M., & Ingham, J. (2018). Seismic behaviour of RC columns flexurally strengthened with FRP sheets and FRP anchors. *Composite Structures*, 203, 382-395.

El-Ghandour, A. A. (2011). Experimental and analytical investigation of CFRP flexural and shear strengthening efficiencies of RC beams. *Construction and Building Materials*, 25(3), 1419-1429.

Lam, L., & Teng, J. G. (2003). Design-oriented stress–strain model for FRP-confined concrete. *Construction and building materials*, 17(6-7), 471-489.